Electronic Supplementary Material (ESI) for Polymer Chemistry.

Supplementary Information

Towards Nanoparticles with Site-Specific Degradability by Ring-Opening Copolymerization Induced Self-Assembly in Organic Medium

Chen Zhu,[†] *Julien Nicolas*[*]

[1] Université Paris-Saclay, CNRS, Institut Galien Paris-Saclay, 92296 Châtenay-Malabry, France

*To whom correspondence should be addressed.

Email: julien.nicolas@u-psud.fr

Tel.: +33 1 46 83 58 53

Table S1. Macromolecular Characteristics of PLMA Macro-CTAs Synthesized by RAFT Polymerization in Anhydrous Toluene at 70 °C for 4 h.

Macro-CTA	RAFT agent	LMA Conv.[a] (%)	$M_{n,SEC}$[b] (g.mol^{-1})	$DP_{n,SEC}$[c]	$Đ$[b]	$M_{n,NMR}$[d] (g.mol^{-1})	$DP_{n,NMR}$[e]
$PLMA_{18}$	CDSPA	49	5 000	18	1.13	4 700	17
	CDB	48	4 900	18	1.19	4 100	15

[a] Determined by ^{1}H NMR. [b] Determined by SEC after precipitation. [c] Calculated according to: $DP_{n,SEC} = (M_{n,SEC} - MW_{RAFT\ agent}) / MW_{LMA}$. [d] Determined by ^{1}H NMR by integrating the signal from the RAFT agent (2H in the α-position to the carboxylic acid of CDSPA at 3.3 ppm and 10H of the aromatic groups of CDB at 7.1-8.1 ppm) and the 2H of PLMA (3.8-4.0 ppm). [e] Determined by ^{1}H NMR according to: $DP_{n,NMR} = (M_{n,NMR} - MW_{RAFT\ agent}) / MW_{LMA}$.

Table S2. Macromolecular and Colloidal Properties of $PLMA_{18}$-*b*-$P(BzMA_{150}$-*co*-MDO) (**L_{18}-Bz_{150}M**) Diblock Copolymer Nanoparticles.

Targeted copolymer	$f_{MDO,0}$	Conv.[a] (%) / Time (h)	F_{MDO}[b]	Opened MDO[c] (%)	$M_{n,NMR}$[d] (g.mol^{-1})	$M_{n,SEC}$[e] (g.mol^{-1})	$Đ$[e]	D_Z[f] (nm)	PSD[f]
L_{18}-Bz_{150}M	0.2	78/20	0.04	75	131 500	36 800	1.9	102	0.18
	0.4	66/20	0.10	66	37 300	45 600	4.3	140	0.34
	0.7	52/20	0.19	75	19 200	46 000	2.5	202	0.26

[a] BzMA conversion determined by ^{1}H NMR. [b] Determined by ^{1}H NMR after precipitation. [c] Determined by integrating the 2H of opened MDO (3.9–4.0 ppm) and the 4H of closed MDO (3.3–3.6 ppm). [d] Determined by ^{1}H NMR by integrating the 2H of MDO (2.5–2.9 ppm) and the 2H of BzMA (4.9–5.1 ppm). [e] Determined by SEC after precipitation. [f] Determined by DLS.

Table S3. Macromolecular and Colloidal Characteristics of **L_{18}-Bz_{150}**, **L_{18}-Bz_{150}MP** (f_{MPDL} = 0.2) and **L_{18}-Bz_{150}M** (f_{MDO} = 0.2) Nanoparticles as Function of the Reaction Time.

Targeted copolymer	Time (h)	Conv.[a] (%)	M_n[b] (g.mol^{-1})	$Đ$[b]	D_z[c] (nm)	PSD[c]
L_{18}-Bz_{150} $f_{CKA,0}$ = 0	5	61	16 200	1.13	232	0.23
	6	66	17 700	1.13	203	0.13
	8	70	18 000	1.14	191	0.11
	20	71	18 400	1.12	179	0.11
L_{18}-Bz_{150}MP $f_{MPDL,0}$ = 0.2	5	39	15 800	1.34	36	0.004
	6	46	17 000	1.35	38	0.04
	8	53	17 200	1.38	41	0.01
	20	76	34 200	1.23	52	0.02
L_{18}-Bz_{150}M $f_{MDO,0}$ = 0.2	5	12	7 000	1.40	43	0.04
	6	14	7 200	1.41	47	0.04
	8	16	7 200	1.43	49	0.07
	20	23	7 500	1.69	149	0.18

[a] BzMA conversion determined by ^{1}H NMR. [b] Determined by SEC. [c] Determined by DLS.

Table S4. Macromolecular Characteristics of P(LMA-*co*-CKA) Macro-CTAs Synthesized by RAFT Polymerization in Anhydrous Toluene at 70 °C for 4 h.

Copolymer[a]	$f_{CKA,0}$	F_{CKA}[b]	Opened CKA[c] (%)	Conv.[d] (%) / Time (h)	$M_{n,NMR}$[e] (g.mol^{-1})	$M_{n,SEC}$[f] (g.mol^{-1})	$Đ$[f]
P(LMA$_{13}$-*co*-BMDO$_{0.7}$)	0.4	0.05	66	39/4	3600	3 600	1.23
P(LMA$_{17}$-*co*-MPDL$_{0.53}$)	0.4	0.03	n.d.	43/4	5700	4 700	1.22

[a] Determined from $M_{n,SEC}$ and F_{MPDL} or F_{BMDO}. [b] Determined by ^{1}H NMR after precipitation. [c] Determined by integrating the 2H of opened BMDO (5.0–5.2 ppm) and the 4H of closed BMDO (4.6–4.8 ppm). [d] LMA conversion determined by ^{1}H NMR. [e] Calculated by ^{1}H NMR by integrating the 2H of the RAFT agent (7.9-8.0 ppm), the 2H of BMDO (2.2–2.4 ppm) or the 2H of MPDL (2.3–2.7 ppm) and the 2H of LMA (3.8–4.0 ppm). [f] Determined by SEC after precipitation.

Table S5. Macromolecular and Colloidal Properties of P(LMA$_{17}$-*co*-MPDL$_{0.53}$)-*b*-PBzMA$_{150}$ (**L$_{17}$MP$_{0.53}$-Bz$_{150}$**) Diblock Copolymer Nanoparticles.

Targeted copolymer	Conv.[a] (%) / Time (h)	$M_{n,NMR}$[b] (g.mol^{-1})	$M_{n,SEC}$[c] (g.mol^{-1})	$Đ$[c]	D_z[d] (nm)	PSD[d]
L$_{17}$MP$_{0.53}$-Bz$_{150}$	73/20	98 600	61 700	1.27	126	0.29

[a] BzMA conversion determined by ^{1}H NMR. [b] Determined by ^{1}H NMR by integrating the 2H of BzMA (4.9-5.1 ppm). [c] Determined by SEC after precipitation. [d] Determined by DLS.

Table S6. Degradation Under Accelerated Conditions of P(LMA-*co*-BMDO) Macro-CTAs [a]

F_{BMDO}[b]	Average consecutive LMA units[c]	Exp. M_n after degradation ($M_{n,exp}$)[d] (g.mol^{-1})	Theo. M_n after degradation ($M_{n,th}^{\infty}$)[e] (g.mol^{-1})	M_n decrease[f] (%)
0.05	19.0	4 350	5 000	-0
0.08	11.5	5 700	3 100	-0
0.09	10.1	2 800	2 700	-26
0.10	9.0	2 200	2 500	-48
0.14	6.1	1 200	1 700	-71
0.24	3.2	600	1 000	-83

[a] Degradation was performed for 1 h at room temperature in THF with 5% KOH in methanol. [b] Determined by ^{1}H NMR after precipitation. [c] Calculated according to: $1/F_{BMDO} - 1$. [d] Determined by SEC ($CHCl_3$ with 0.1% v/v TFA). [e] Calculated according to: $MW_{LMA} \times (1 / F_{BMDO} - 1) + MW_{BMDO}$. [f] M_n decrease after hydrolytic degradation of the purified copolymers calculated according to: (exp. $M_{n,SEC}$ − initial $M_{n,SEC}$) / initial $M_{n,SEC}$.

Table S7. Macromolecular Characteristics of P(LMA-*co*-CKA) Macro-CTA Synthesized by RAFT Polymerization in Anhydrous Toluene at 90 °C for 4 h

Macro-CTA[a]	$f_{CKA,0}$	F_{CKA}[b]	Opened CKA[c] (%)	Conv.[d] (%) / Time (h)	$M_{n,NMR}$[e] (g.mol^{-1})	$M_{n,SEC}$[f] (g.mol^{-1})	$Đ$[f]	M_n decrease[g] (%)
P(LMA$_{28}$-*co*-MPDL$_{2.1}$)	0.20	0.07	n.d.	78/4	8500	7 600	1.24	-38
P(LMA$_{20}$-*co*-BMDO$_{2.2}$)	0.40	0.10	87	64/4	7800	5 700	1.38	-40

[a] Determined from $M_{n,SEC}$ and F_{MPDL} or F_{BMDO}. [b] *D*etermined by ^{1}H NMR after precipitation. [c] Determined by integrating the 2H of opened BMDO (5.0–5.2 ppm) and the 4H of closed BMDO (4.6–4.8 ppm). [d] LMA conversion determined by ^{1}H NMR. [e] Calculated by ^{1}H NMR by integrating the 2H of the RAFT agent (7.9-8.0 ppm), the 2H of BMDO (2.2–2.4 ppm) or the 2H of MPDL (2.3–2.7 ppm) and the 2H of LMA (3.8–4.0 ppm). [f] Determined by SEC after precipitation. [g] Determined according to: (exp. $M_{n,SEC}$ – initial $M_{n,SEC}$) / initial $M_{n,SEC}$.

Table S8. Macromolecular and Colloidal Properties of P(LMA-*co*-CKA)-*b*-P(BzMA-*co*-CKA) Diblock Copolymer Nanoparticles.

Macro-CTA	Core CKA	$f_{CKA,0}$	F_{CKA}[a]	Conv.[b] (%) / Time (h)	$M_{n,NMR}$[c] (g.mol^{-1})	$M_{n,SEC}$[d] (g.mol^{-1})	$Đ$[d]	D_z[e] (nm)	PSD[e]
P(LMA$_{20}$-*co*-BMDO$_{2.2}$)	-	0	-	79/16	119 300	76 900	1.57	166	0.25
P(LMA$_{20}$-*co*-BMDO$_{2.2}$)	BMDO	0.40	0.12	52/16	18 600	13 200	1.60	61	0.01
P(LMA$_{28}$-*co*-MPDL$_{2.1}$)	-	0	-	58/16	87 900	36 200	1.13	96	0.10
P(LMA$_{28}$-*co*-MPDL$_{2.1}$)	MPDL	0.40	0.15	50/16	23 900	18 000	1.35	115	0.22

[a] *D*etermined by ^{1}H NMR after precipitation. [b] LMA conversion determined by ^{1}H NMR. [c] Determined by ^{1}H NMR by integrating the 2H of BMDO (2.2–2.4 ppm) or 2H of MPDL (2.3-2.7 ppm) and the 2H of BzMA (4.9-5.1 ppm). [d] Determined by SEC after precipitation. [e] Determined by DLS.

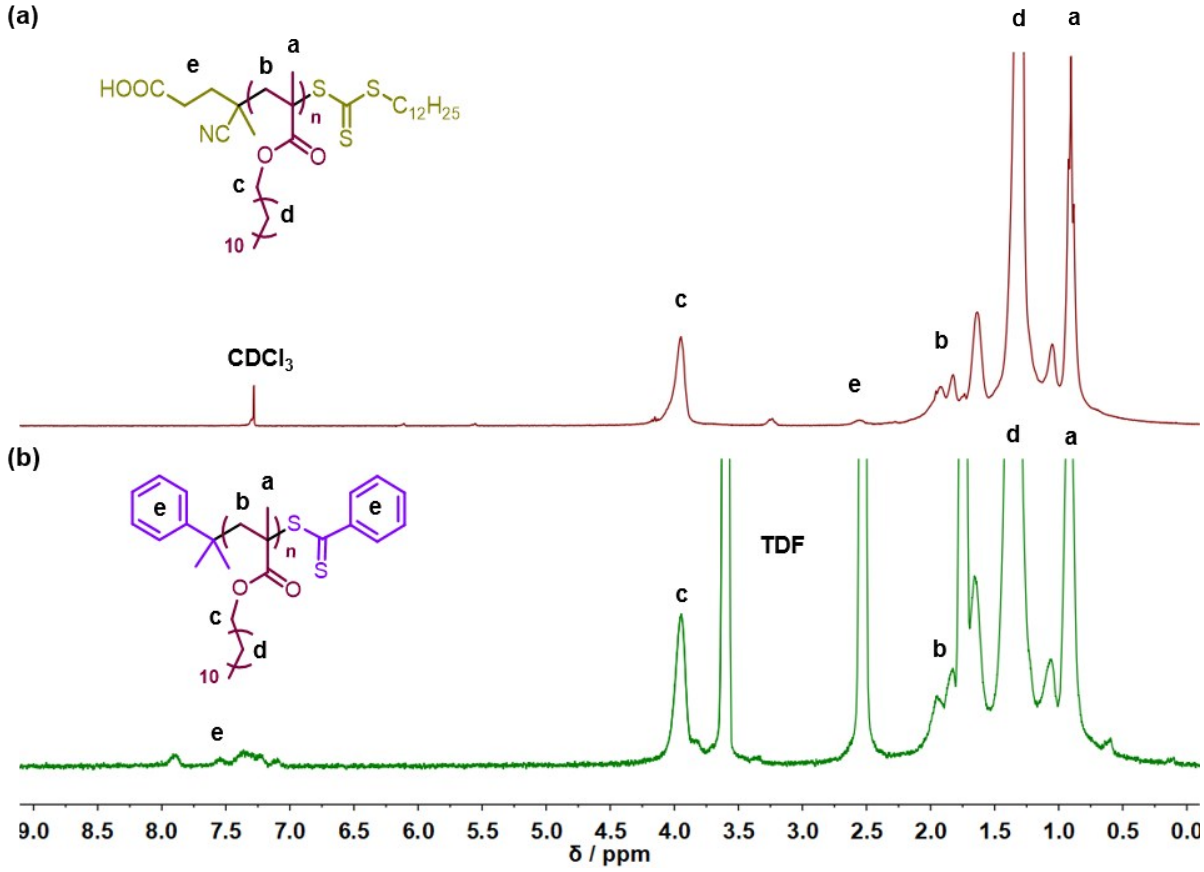

Figure S1. ^{1}H NMR spectra in the 0–9 ppm region of: (a) $PLMA_{18}$-CDSPA in $CDCl_3$ and (b) $PLMA_{18}$-CDB in tetrahydrofuran-d_8, TDF.

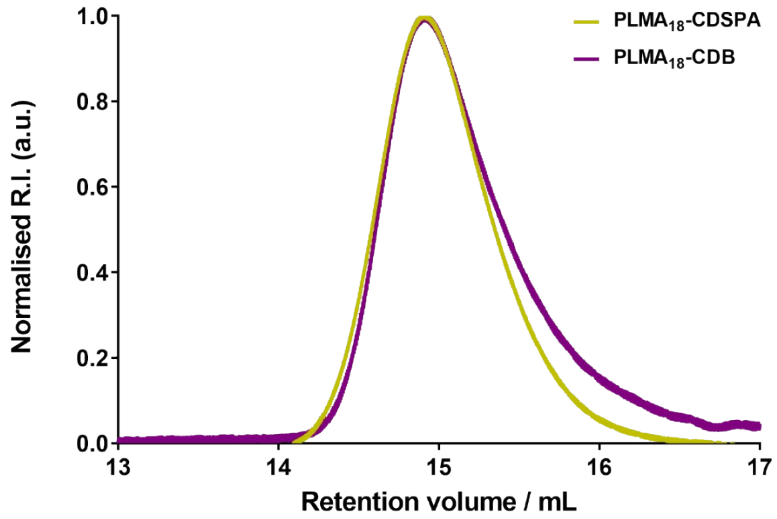

Figure S2. SEC chromatograms ($CHCl_3$) of $PLMA_{18}$-CDSPA and $PLMA_{18}$-CDB.

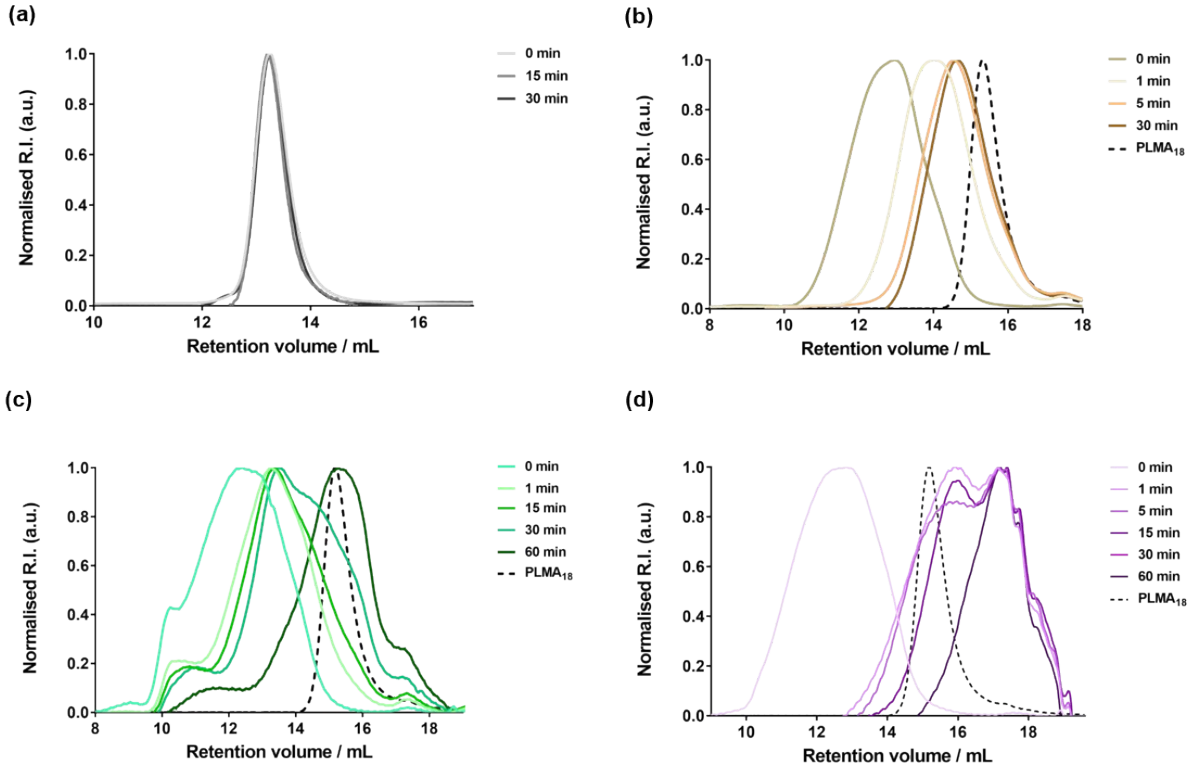

Figure S3. Evolution of the SEC chromatograms ($CHCl_3$, 0.1% v/v TFA) with time during the degradation under accelerated conditions (THF/MeOH, KOH 2.5%) of $\mathbf{L_{18}Bz_{150}M}$ copolymers

as function of the MDO content: (a) $F_{MDO} = 0$; (b) $F_{MDO} = 0.04$; (c) $F_{MDO} = 0.10$ and (d) $F_{MDO} = 0.19$.

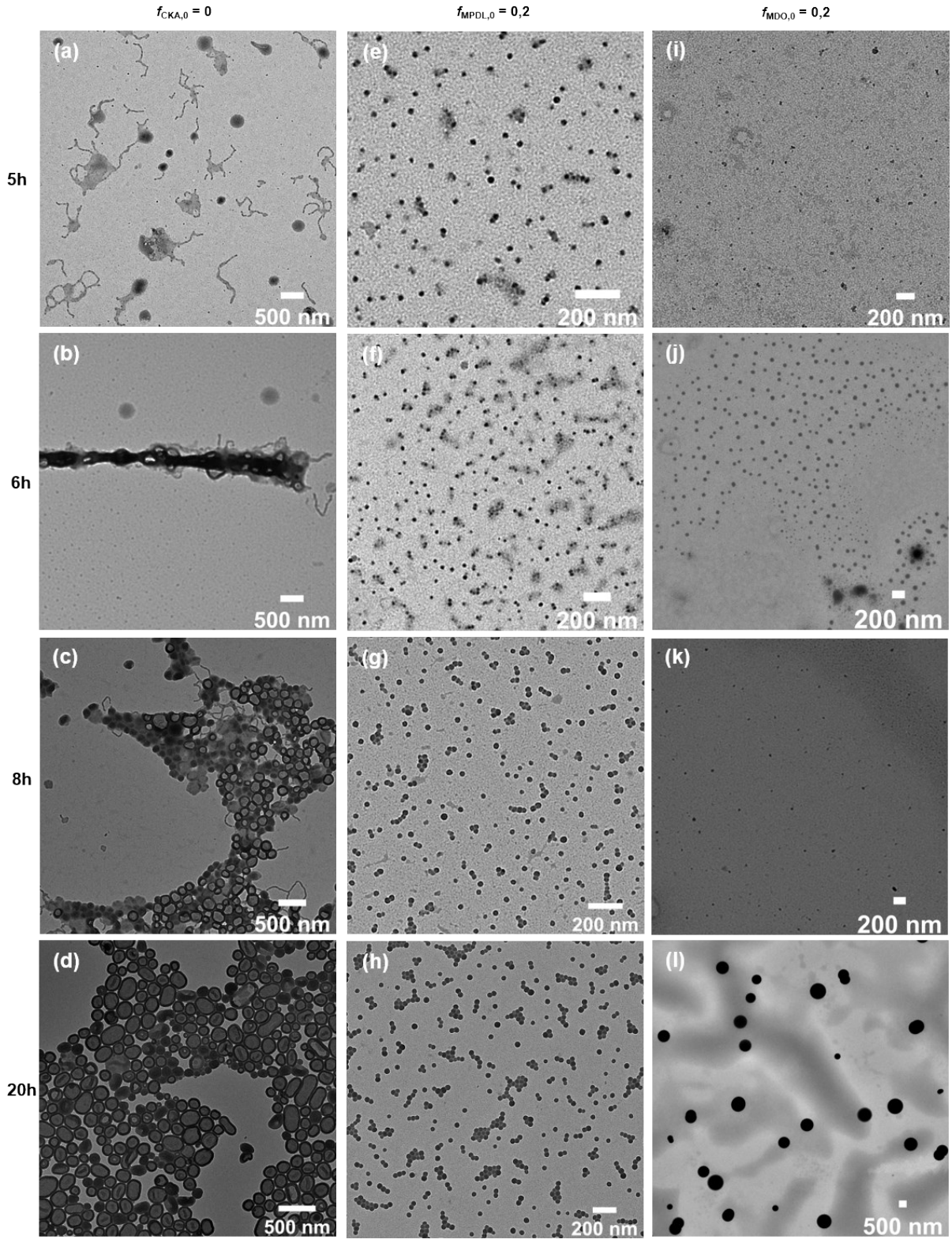

Figure S4. Representative TEM images of **L_{18}-Bz_{150}**, **L_{18}-Bz_{150}MP** (f_{MPDL} = 0.2) and **L_{18}-Bz_{150}M** (f_{MDO} = 0.2) nanoparticles with the reaction time.

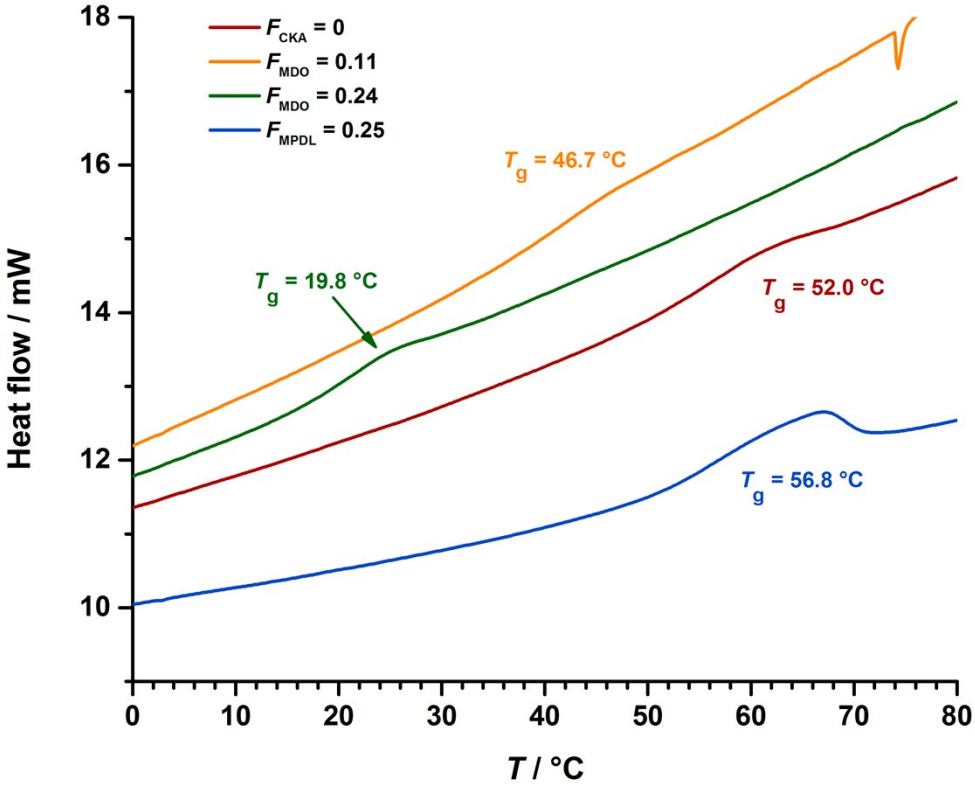

Figure S5. DSC measurements performed on **L_{18}-Bz_{150}** (F_{CKA} = 0), **L_{18}-Bz_{150}MP** (F_{MPDL} = 0.25), **L_{18}-Bz_{150}M** (F_{MDO} = 0.19 and F_{MDO} = 0.10).

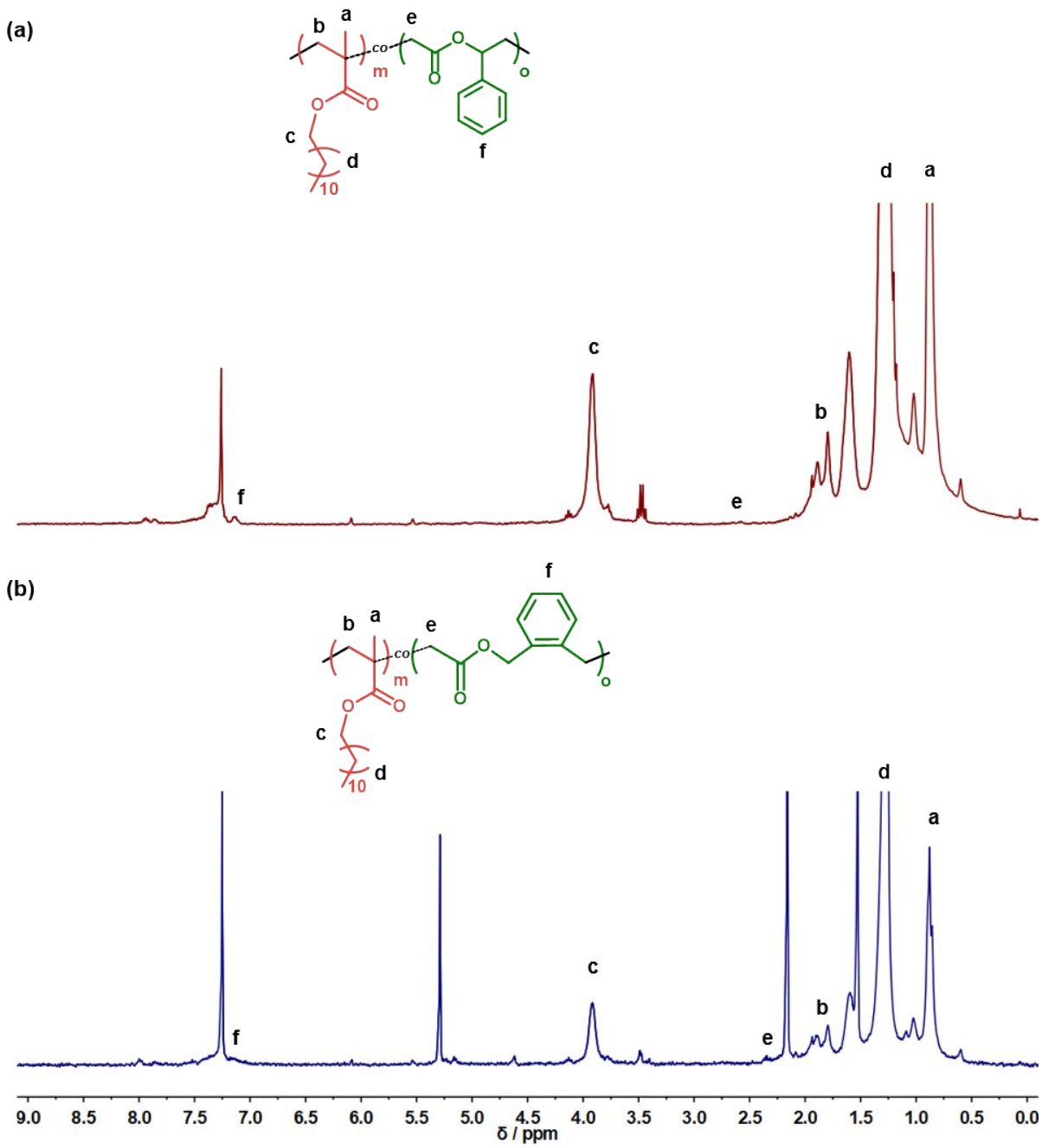

Figure S6. ^{1}H NMR spectra in $CDCl_3$ in the 0–9.0 ppm region of: (a) P(LMA_{17}-*co*-$MPDL_{0.53}$) and (b) P(LMA_{13}-*co*-$BMDO_{0.7}$) macro-CTAs.

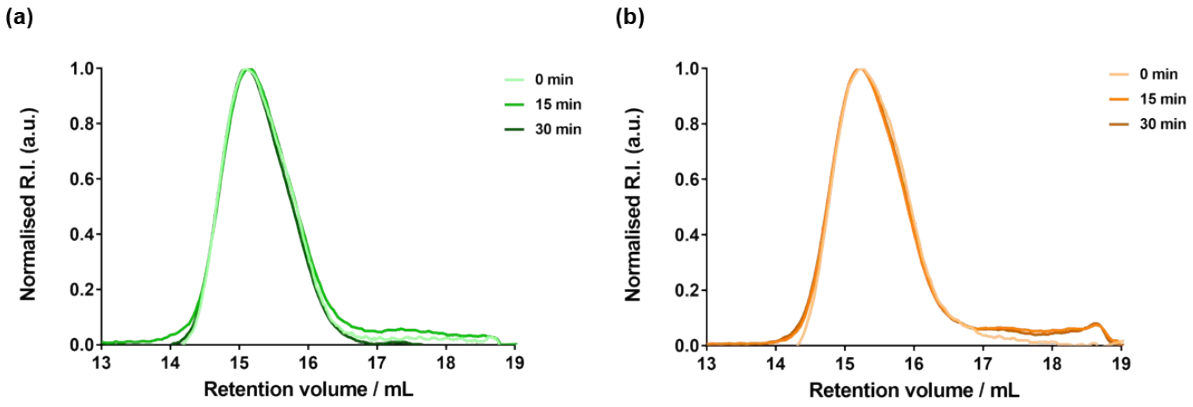

Figure S7. Evolution of the SEC chromatograms ($CHCl_3$) at different time during the degradation under accelerated conditions (THF/MeOH, KOH 2.5%) of: (a) P(LMA_{17}-*co*-$MPDL_{0.53}$) and (b) P(LMA_{13}-*co*-$BMDO_{0.7}$).

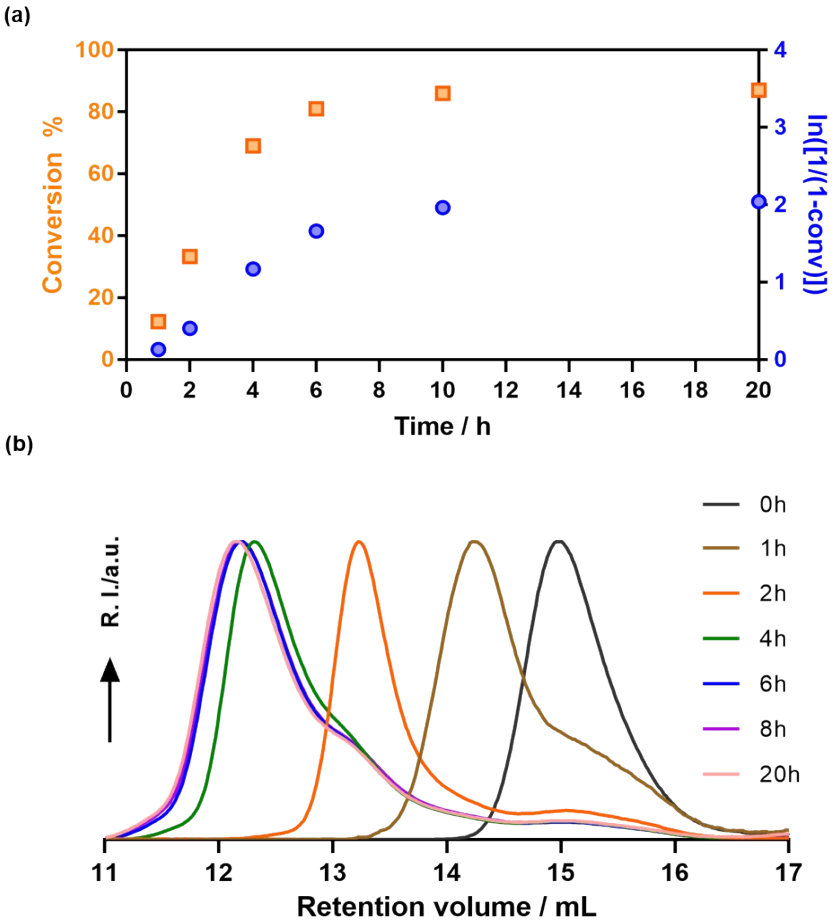

Figure S8. Synthesis of $\mathbf{L_{17}MP_{0.53}\text{-}Bz_{150}}$ diblock copolymers by rROPISA in heptane at 90°C: (a) Evolution of BzMA conversion and logarithmic conversion vs. time plots and (b) evolution of the SEC chromatograms ($CHCl_3$) with time using normalised RI values.

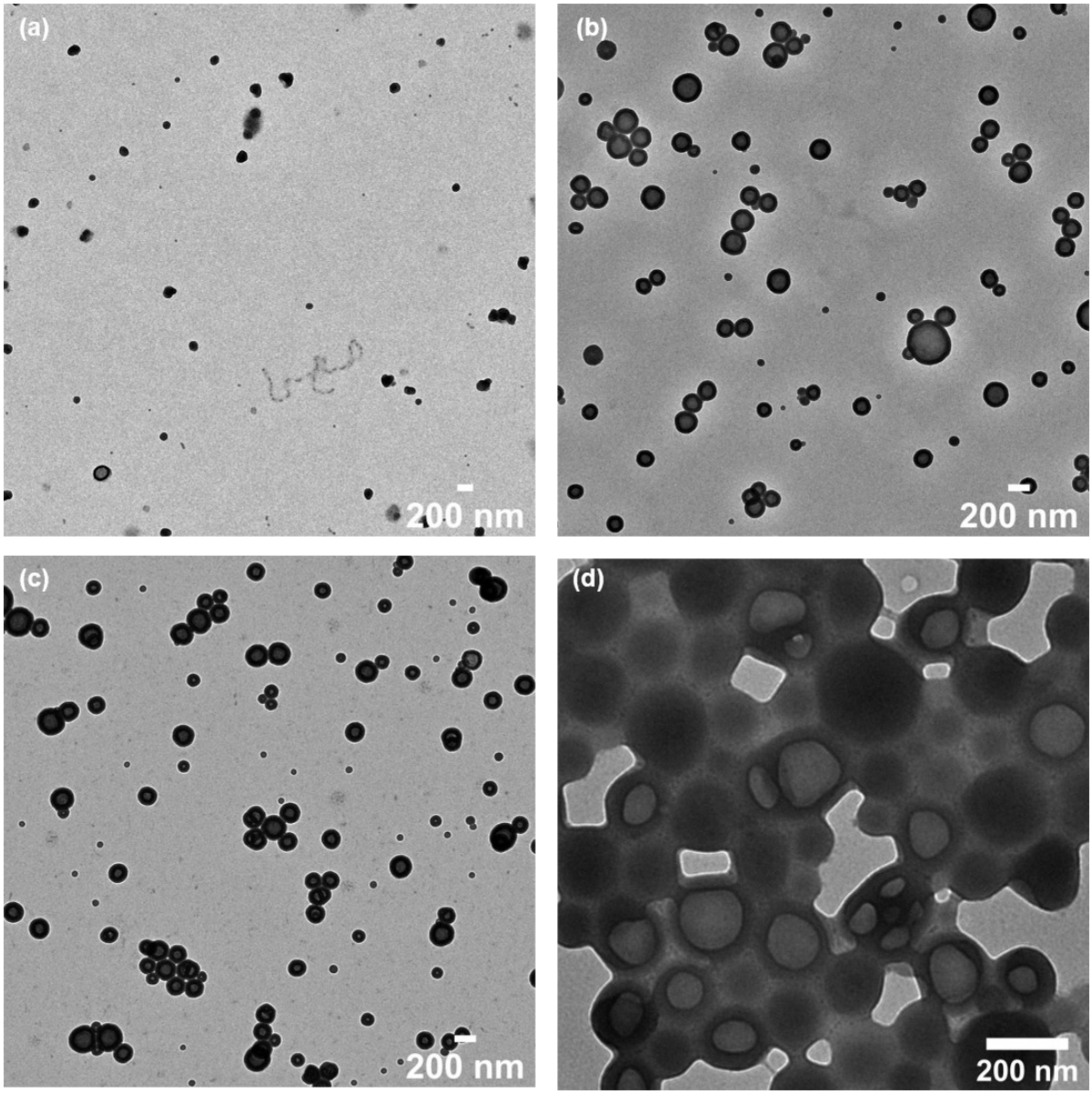

Figure S9. Representative TEM images of $\mathbf{L_{17}MP_{0.53}\text{-}Bz_{150}}$ nanoparticles at different time points: (a) 2h; (b) 4h; (c) 8h and (d) 20h.

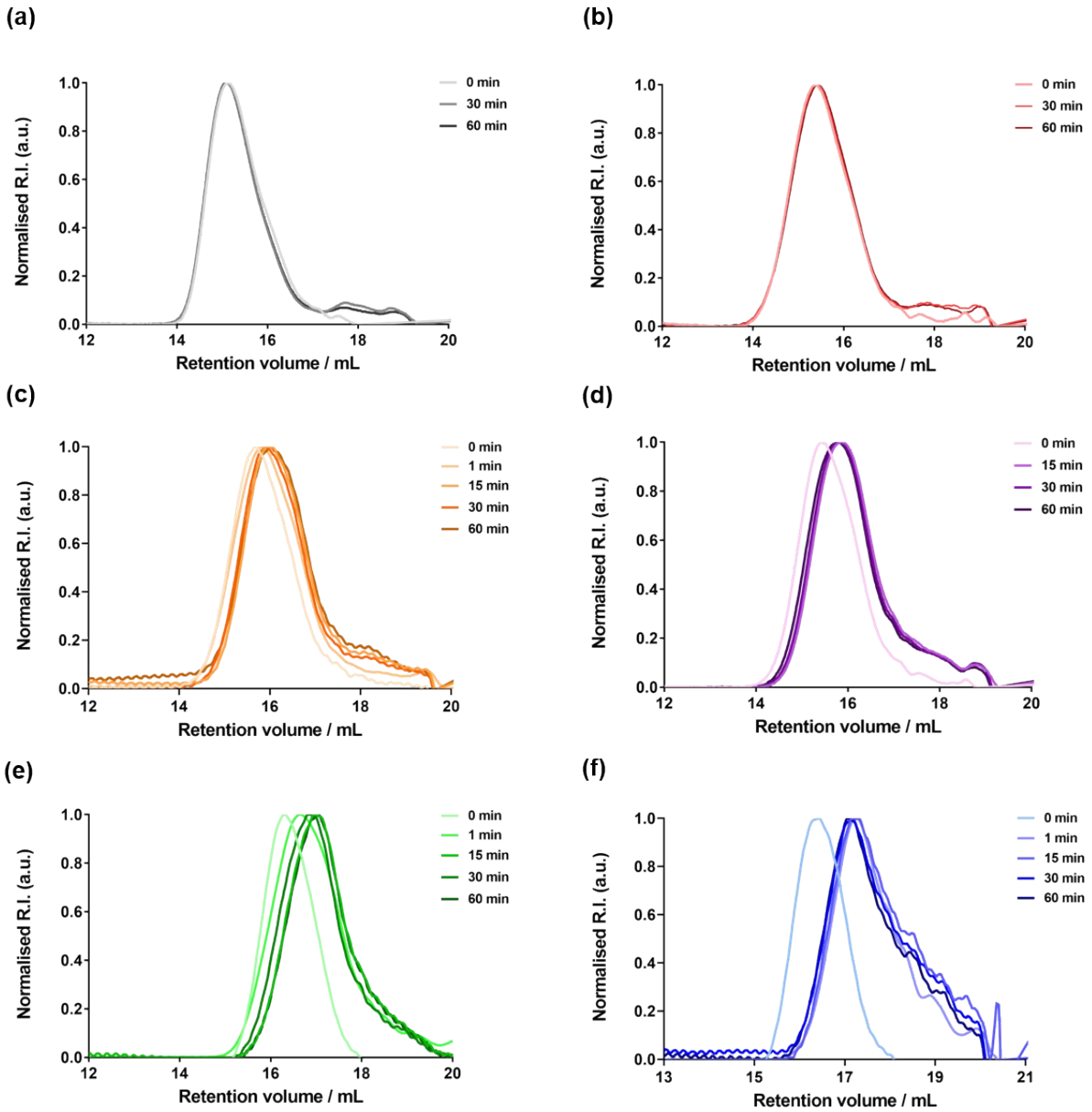

Figure S10. Evolution of the SEC chromatograms ($CHCl_3$ with 0.1% v/v TFA) at different time during the degradation under accelerated conditions (THF/MeOH, KOH 2.5%) of P(LMA-*co*-BMDO) macro-initiator (a) $F_{BMDO} = 0.05$, (b) $F_{BMDO} = 0.08$, (c) $F_{BMDO} = 0.09$, (d) $F_{BMDO} = 0.10$, (e) $F_{BMDO} = 0.14$, (b) $F_{BMDO} = 0.24$.

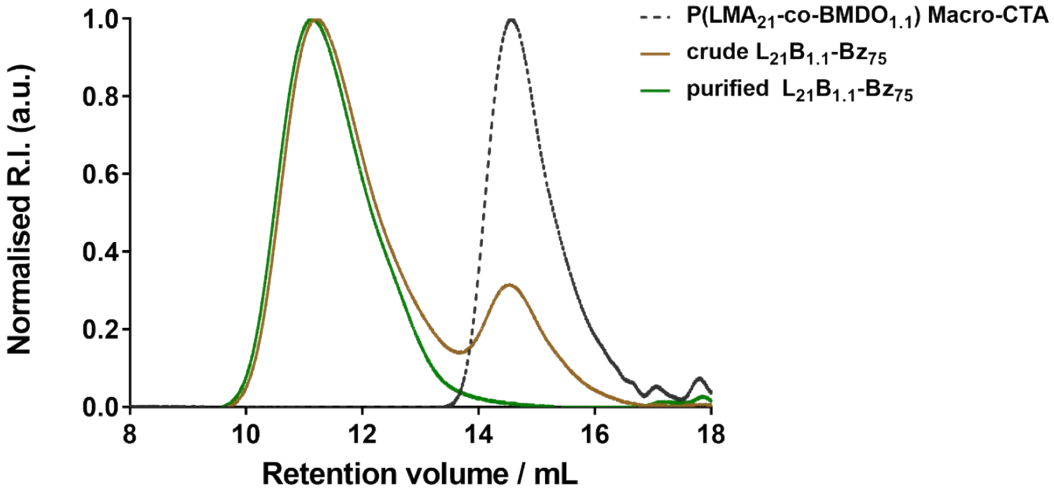

Figure S11. SEC chromatograms ($CHCl_3$) of P(LMA_{21}-*co*-$BMDO_{1.1}$) macro-CTA and of **$L_{21}B_{1.1}$-Bz_{75}** copolymers before and after purification.

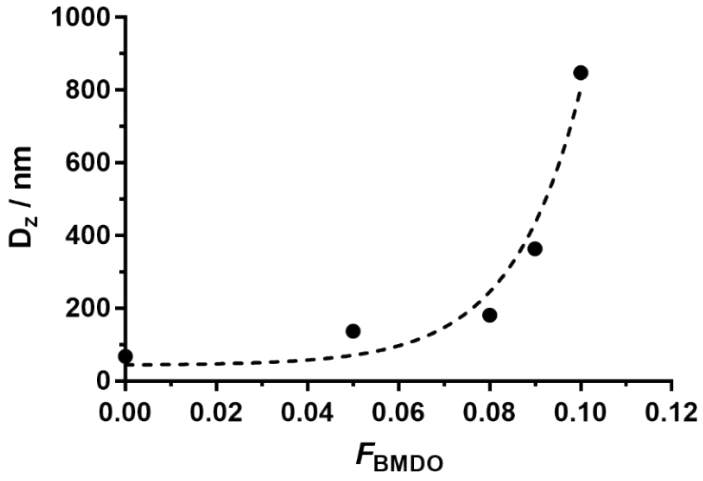

Figure S12. Evolution of the intensity-average diameter (D_z) of P(LMA-*co*-BMDO)-*b*-$PBzMA_{75}$ nanoparticles with F_{BMDO}.

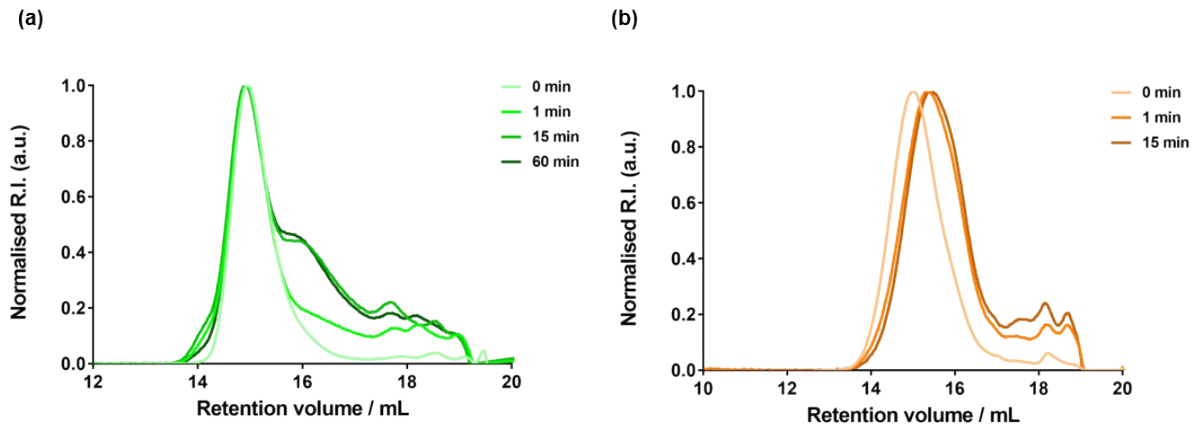

Figure S13. Evolution of the SEC chromatograms ($CHCl_3$) at different time during the degradation under accelerated conditions (THF/MeOH, KOH 2.5%) of: (a) P(LMA_{20}-*co*-$BMDO_{2.2}$) and (b) P(LMA_{28}-*co*-$MPDL_{2.1}$).

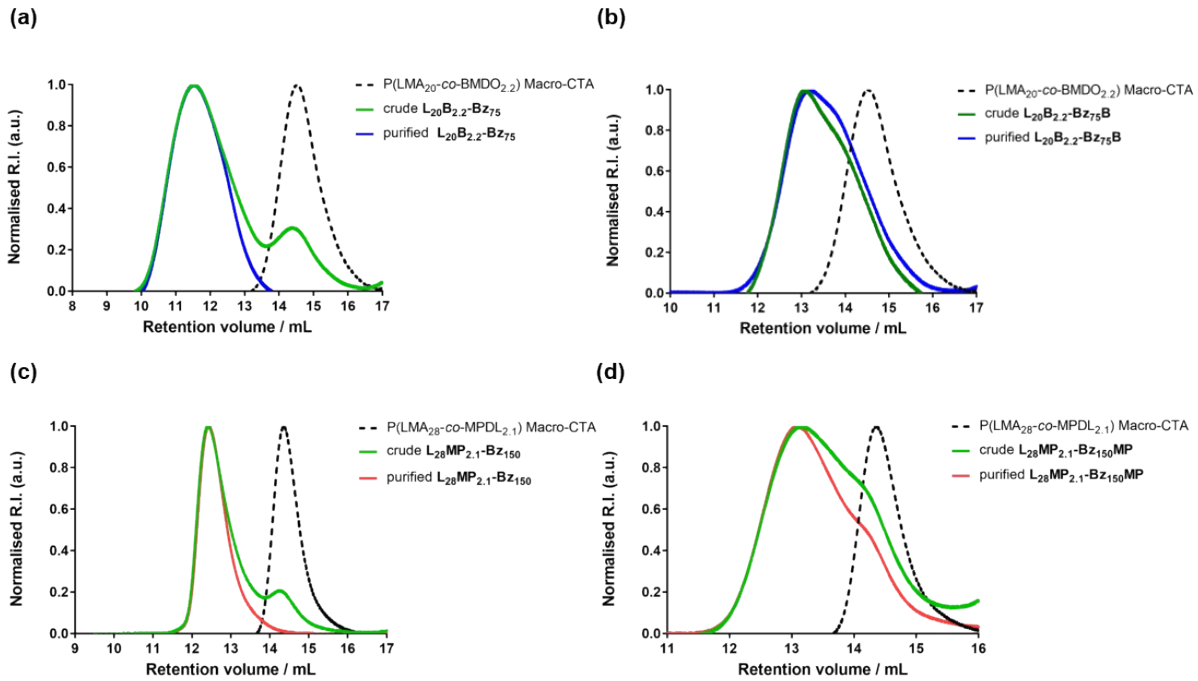

Figure S14. Evolution of the SEC chromatograms ($CHCl_3$) obtained after chain extension by rROPISA from: (a) P(LMA_{20}-*co*-$BMDO_{2.2}$) with BzMA; (b) P(LMA_{20}-*co*-$BMDO_{2.2}$) with BzMA and BMDO (f_{BMDO} = 0.4); (c) P(LMA_{28}-*co*-$MPDL_{2.1}$) and (d) P(LMA_{28}-*co*-$MPDL_{2.1}$) and MPDL (f_{MPDL} = 0.4).

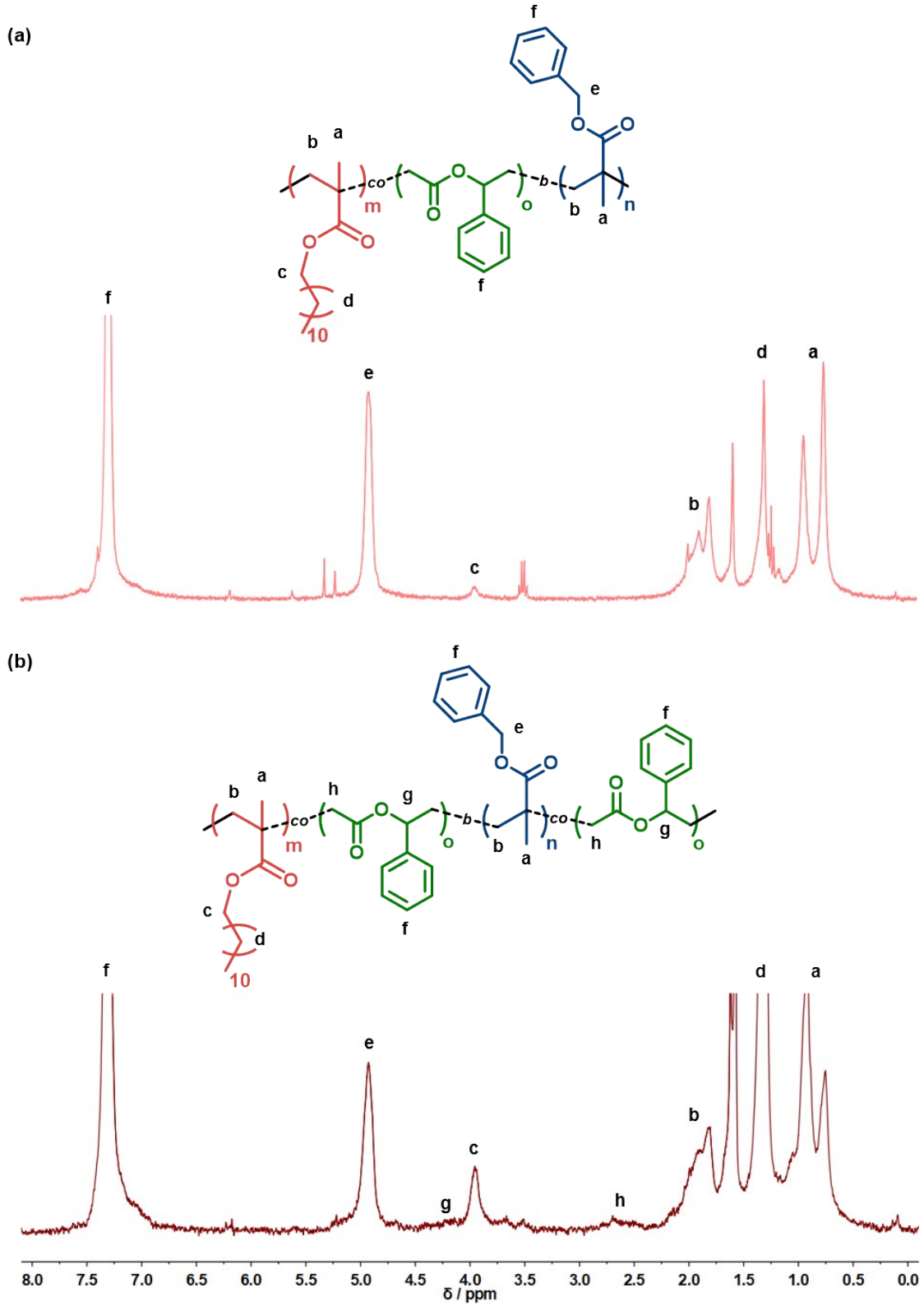

Figure S15. ^{1}H NMR spectra in $CDCl_3$ in the 0–8 ppm region of: (a) **$L_{28}MP_{2.1}$-Bz_{150}** and (b) **$L_{28}MP_{2.1}$-Bz_{150}MP** copolymers. Note that protons belonging to MPDL are no longer visible for **$L_{28}MP_{2.1}$-Bz_{150}**.

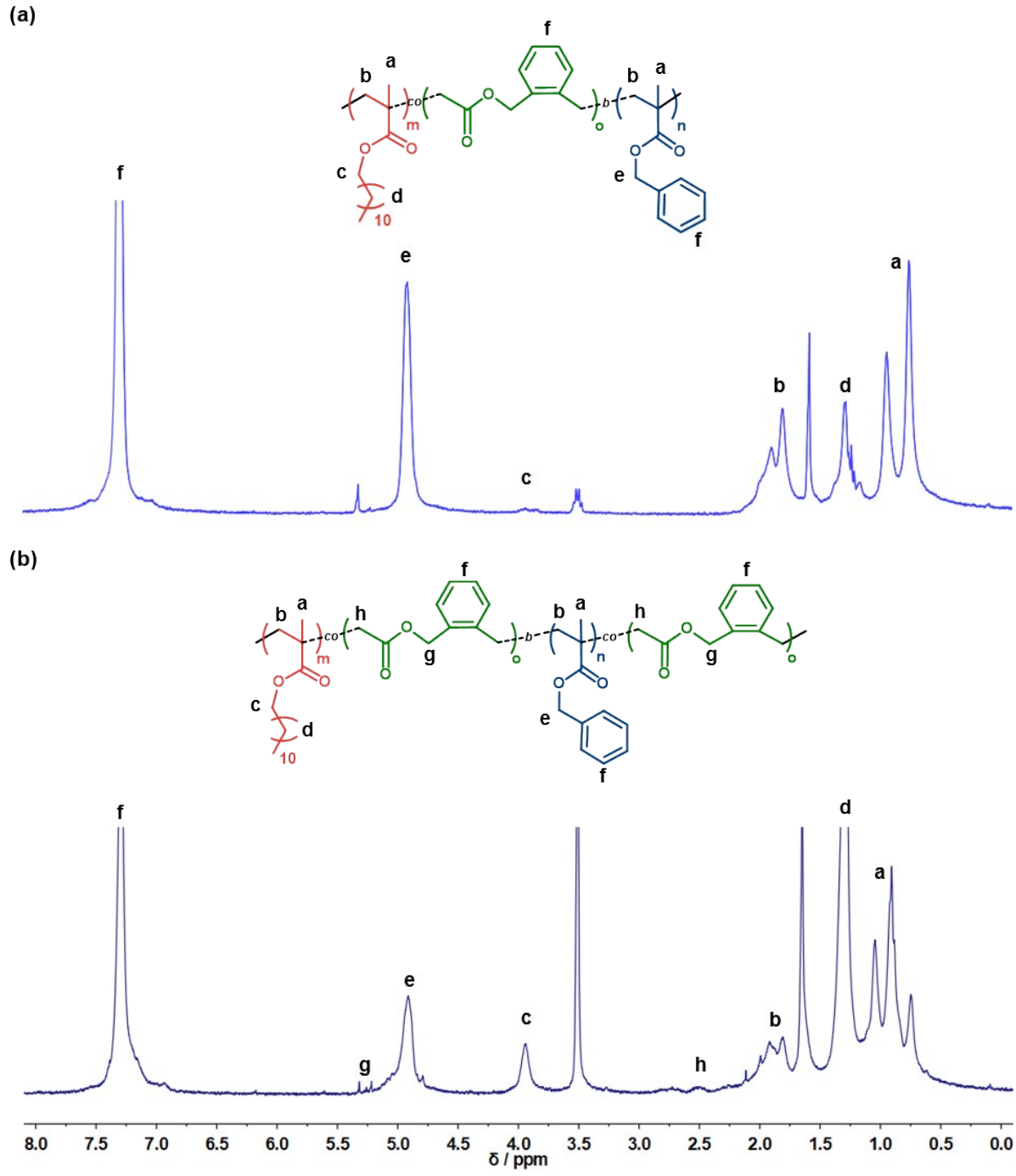

Figure S16. ^{1}H NMR spectra in $CDCl_3$ in the 0–8 ppm region of: (a) **$L_{20}B_{2.2}$-Bz_{75}** and (b) **$L_{20}B_{2.2}$-Bz_{75}B** copolymers. Note that protons belonging to BMDO are no longer visible for **$L_{20}B_{2.2}$-Bz_{75}**.